Oxygen and Glucose Transportation and Distribution on 3D Osteochondral Scaffold in Silico Model

Ziyu Liu[1,2] · Hao Huang[2,3] · Jingying Yang[2] · Maryam Tamaddon[1] · Haoyu Wang[1] · Yingying Gu[1] · Zhenyun Shi[3] · Chaozong Liu[1]

Abstract

Nutrients supply especially like nutrients and oxygen play vital role in tissue engineering process. It is found that tissue could not grow very well in the middle of the scaffold because few nutrients could transport to the middle. Nutrient limitations would reduce cell proliferation and differentiation. In that case, there is urgent need to understand the nutrient distribution for both in vitro and in vivo study, as no technology is able for researchers to observe the nutrients transport during those process. In this paper, a numerical model coupling with VOF (volume of fluid) model and species transport model together for predicting the distribution of oxygen and glucose in the scaffold after implantation in to the site is developed. Comparing with our previous in vivo tests, the regenerated tissue distribution has a similar trend as oxygen distribution rather than glucose. The reported scaffold manufactured by additive manufacturing provided a good interconnected structure which facilitated the nutrient transportation in the scaffold. Considering nutrient transportation, this numerical model could be used in better understanding the nutrients transportation in the scaffold, and leading to a better understanding of tissue formation in the scaffold.

Keywords Nutrient transport · Scaffold · Nutrient distribution · Computational fluid dynamic · Discrete phase model

1 Introduction

Nutrient supply is a critical factor for tissue engineering success. Cells require nutrients and oxygen to survive. In vitro studies have shown that nutrient concentration in the scaffold is decreasing towards its center due to the consumption of nutrients by the cells and the relatively slow supply by diffusion. Only cells up to a distance of approximately 200 μm have access to sufficient nutrients [1]. This results in nutrient limitations for cells that are further away from the engineered tissue surface, and thus reduced cell proliferation or non-optimal conditions for new matrix production. However, there is an urgent need to understand the nutrient distribution for both in vitro and in vivo studies, as no technology is currently available for researchers to observe the nutrient transport during these processes.

In the tissue engineering field, scaffolds act as a 3D structure for supporting cell growth, providing sufficient mechanical support and provide an extracellular matrix environment for tissue regeneration [1–5]. To achieve success in tissue engineering, nutrient transports into the interior scaffold should be well investigated as it is one of the most significant factors in the success for a scaffold [6, 7]. In thick scaffolds, cells at central region lack a sufficient nutrient supply of glucose and oxygen due to a slow diffusion rate [8]. This effect has been explored in many tissue engineering systems where cell growth is restricted to only few hundred microns from the blood vessel [9–11] Waste products like CO2 and lactate, could also accumulate in the scaffold which would lead to cell growth suppression and heterogeneous distribution [12, 13]. The effect of liquid transportation on cell growth has been rarely studied and should be reviewed and reported in more depth.

✉ Chaozong Liu
chaozong.liu@ucl.ac.uk

[1] Division of Surgery and Interventional Science, Royal National Orthopaedic Hospital, University College London, Stanmore, London HA7 4LP, UK

[2] Beijing Advanced Innovation Centre for Biomedical Engineering, School of Engineering Medicine, Beihang University, Beijing 100083, China

[3] School of Mechanical Engineering and Automation, Beihang University, Beijing 100191, China

Although nutrient transportation plays a vital role in tissue regeneration, it remains difficult to experimentally investigate this dynamic process. Two of the main mechanisms governing nutrient transportation are convection and diffusion [14]. Convection is a faster mass transport method due to bulk fluid motion and diffusion is a significantly slower transport mechanism due to its reliance upon a concentration gradient. In a bioreactor system, the solution transportation is usually generated by external sources called forced convection in most bioreactor systems [15], the flow speed caused by external sources is far higher than the diffusion speed, meaning that that the transportation type in most bioreactor systems mostly relies upon convection rather than diffusion. Unlike normal solutions for cultivating cells, bone marrow is a semi-solid tissue [16] which is hard to mimic experimentally. During in vivo and in vitro tests, there are no techniques which are able to monitor the entire biosystem including temperature, cell density, bone marrow speed, nutrients transportation and density. Computational analysis provides a promising method to understand the tissue regeneration process from cell seeding to tissue regeneration [17].

Xu et al., investigated how fluid velocity and shear stress influenced cell seeding in a bioreactor system with randomly structured scaffolds. The fluid velocity was set between 0.26 and 0.64 mm/s which was able to predict bio-performance in bioreactor as the nutrient transportation type was largely dependent on convection [18]. In consideration of diffusion speed of glucose, Edward et al. [19] explored the effects of flow-induced nutrient transport and fluid perfusion for cells on scaffolds in a rotational bioreactor during dynamic bioreactor cultivation. Alireza et al. [8] developed a numerical model to better understand the relationship between oxygen supply and cell density in a channelled scaffold.

Most of the recent studies creating numerical models have been used for predicting cell density, nutrient distribution or fluid performance (shear stress). Few researchers are working on developing models for predicting in vivo performance based on limited in vivo or clinical trial experimental data. The critical difference in the transportation of cells and nutrients in the bioreactor when compared to the body is that forced convection is the principal factor in bioreactor while concentration gradient-dependent diffusion is the principal factor in vivo. To achieve a highly accurate numerical model for tissue engineering, every step should be well considered—(1) cell migration with bone marrow and colonies into the scaffold (2) nutrient transportation for cell proliferation, differentiation and migration; (3) new tissue formation [20]. During the whole period, many factors should be quantified such as cell density, oxygen and glucose transport, other nutrients, cell-material interactions, cell–cell signalling molecules and growth factors etc [19, 21].

Based on previous studies focussed on improving the model accuracy for predicting scaffold recruitment of BMSCs using the Stanton-Rutland model to simulate cell-material interaction [22], a model was designed for predicting the nutrients distribution in an in vivo system and quantify nutrient absorption of attached cells on the scaffold. According to previous in vivo tests from the micro-CT and CT image analysis, it was found that trabecular bone regenerated more on the edge of the scaffold than in the centre [22, 23]. A decreasing bone formation rate was found from bottom to the top of the scaffold. In this numerical model, the relationship between the regenerated tissue distribution on the scaffold and the nutrient distribution would be investigated, considering oxygen and glucose. To simplify the model, glucose and oxygen are investigated for the nutrient transport as they are key substrates in cell growth process.

2 Materials and Methods

2.1 Scaffold Characteristics and In Vivo Tests

Osteochondral scaffold is made by 3 layers which composited by PLA, PLGA and pure titanium shown in Fig. 1 [22]. According to our previous research, only pure titanium layer aims for osteogenesis which is infiltrated in the bone marrow. Titanium layer is manufactured by EOS 290 3D printer which geometry is designed by cutting 10 degrees of the 8 mm diameter and 6 mm height column structure which means that it is truncated cone with 8 mm diameter on the top surface and 5.9 mm on the bottom surface. Each beam is 0.5 diameter and they cross linked together forming a cubic structure [22]. A critical-sized truncated cone osteochondral defect was drilled. Before put scaffold into the hole, a water gun is used to flush the hole. After being implanted into the 5 sheep condyle, all sheep recovered well and no post-operative complications were found during the period. According to the high-resolution X-ray's image analysis, it

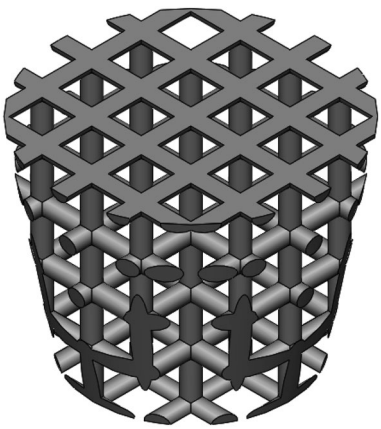

Fig. 1 Osteochondral scaffold titanium layer [22]

is found that new bone tissues prefer to regenerate on the scaffold surface which might cause by unevenly nutrient distribution. The regenerated bone tissue showed a gradual growth trend from scaffold edge to the middle, the growth rate in the scaffold middle is considerable [22]. As there is no experimental facilities could help researchers to observe the process, computational fluid dynamic is used to solve this issue.

2.2 Simulation Computational Framework

Blood and air is governed by the continuity equation and Navier–Stokes equations. The conservation equation of nutrients (glucose and oxygen) takes the following general form:

$$\frac{\partial}{\partial t}\rho Y_i + \nabla \cdot \rho \vec{v} Y_i = -\nabla J_i + R_i \quad (1)$$

This convection–diffusion conservation equation of species transport is to calculate the local mass fraction of each species and Y_i represents the i species. As this simulation solver is pressure based, R_i, the rate of production of species, at inlets consists of both convection and diffusion components. $\vec{J}_i$ represents the diffusion flux of nutrients species due to their concentration gradients. In general, there are 2 different form to describe diffusion which are laminar flow form and turbulent flow form for mass diffusion flux. It used Fick's law to calculate it and the laminar flow form for diffusion flux could be written as:

$$\vec{J}_i = -\rho D_{i,m} \nabla Y_i - D_{T,i} \frac{\nabla T}{T} \quad (2)$$

where $D_{i,m}$ defined as mass diffusion coefficient for nutrients in the mixture and $D_{T,i}$ represents the thermal diffusion coefficient. The turbulent flow form for diffusion flux could be written as:

$$\vec{J}_i = -\rho D_{i,m} \nabla Y_i + \frac{\mu_t}{\mathrm{Sc}_t} - D_{T,i} \frac{\nabla T}{T} \quad (3)$$

where μ_t is the turbulent viscosity and Sc_t is the Schmidt number which is dimensionless value used to characterize flow with mass and momentum diffusion convection process. The Schmidt number is defined as:

$$\mathrm{Sc}_t = \frac{\nu}{D} = \frac{\mu}{\rho D} \quad (4)$$

where ν is the kinematic viscosity (m^2/s), D is the mass diffusivity (m^2/s), μ is the dynamic viscosity (kg/m s or N s/m^2 or

$$\vec{J}_i = -\rho D_{i,m} \nabla Y_i \quad (5)$$

2.3 Solving Process and Boundary Conditions

Nutrients transportation process at initial stage of surgery was simulated by ANSYS Fluent coupling the species including cell and bone marrow by species transport model and volume Volume of Fluid method (VOF) model. As the blood and air are two immiscible fluids that have clearly interface, Volume of Fluid method is used to solve the blood injection process. Volume of Fluid (VOF) model is the free-surface modelling which is used to track and locate the free surface. Tracking the interface between immiscible flows is calculated by the solution of the continuity equation of the volume fraction of the phases. As scaffold was pressed into the defect after continuing washed the osteochondral defect, nutrients transportation starts at the time when stop flushing. The blood fulfilled the whole void space of the defect is calculated by VOF model shown in Fig. 2.

In initial condition, bone marrow set as non-Newtonian fluid was fulfilled the system governed by non-Newtonian power law. The surrounding faces on the side and bottom are the inlet surfaces that support glucose and oxygen with 3 μm/s diffusion. As bone marrow is a semi-solid tissue and it shows fluid property at the beginning and solidifies afterwards, it is assumed that the bone marrow act as fluid until 2000s.The parameters of nutrients and fluid is shown in Table 1.

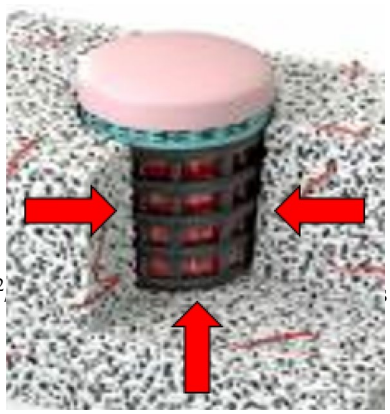

kg/m s) and p is the density of fluid (kg/m^3). In this solving process, thermal gradient would not be occurred during species diffusion. In that case, diffusion flux could be simplified written as:

Fig. 2 Blood fulfilled the whole void space of the defect

Table 1 Model parameters of nutrients and boundary conditions

Descriptions	Values
Glucose concentration	4.5 g/cm^3
Glucose diffusivity in the fluid	9.2×10^{-7} cm^2/s
Glucose inlet speed	3 μm/s
Oxygen concentration	0.1 mol/m^3
Oxygen diffusivity in the fluid	2×10^{-9} cm^2/s
Oxygen inlet speed	3 μm/s
Consistency index—blood	0.017
Power-Law Index—blood	0.708
Minimum and maximum viscosity Limit	0.001 and 0.1
Density of blood (with bone marrow)	1.05 g/cm^3

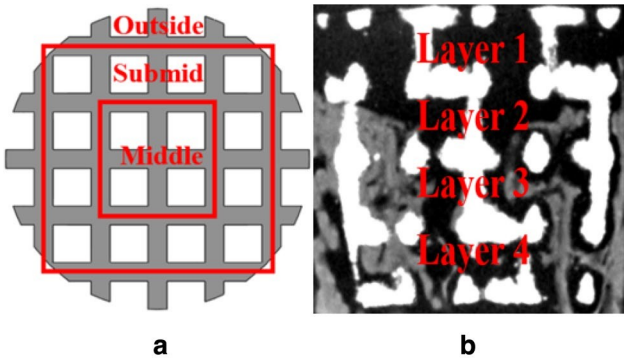

Fig. 3 The definition area of the scaffold in horizontal and vertical view

3 Results

3.1 Oxygen and Glucose Distribution in Horizontal Level

According to the horizontal view shown in Figs. 3a, 4 showed that nutrients distributed more on the outside area and there is a gradual decrease trend from outside to the middle of the scaffold. As the inlet face are near the outside area, the nutrients on the outside area will have the most nutrients concentration and the rate would not show a big different.

As for the oxygen and glucose concentration in submid and middle area, they had a rapid increasing from the beginning until 1200 s. After that, the concentration of glucose increased slowly and there is no significant different between 1600 and 2000s nutrients concentration percentage in all 3 areas. However, with same increasing trend in the submid area, oxygen in the middle areas showed a continuing increasing rate until 2000s, given in Fig. 4.

3.2 Oxygen and Glucose Distribution in Vertical Level

According to the vertical view shown in Fig. 3b, the bottom layer showed the most nutrient concentration comparing to all the other layers shown in Fig. 5a and b. After 2000s, the glucose weight of layer 4 is 0.004% higher than the weight of layer 1. The oxygen of layer 4 is 0.0009% higher than the bottom layer 1. As for oxygen volume percentage, all layers had a gradual increasing speed until 1200 s. After that, top two layers (Layer 3,4) seems like the oxygen is saturate which there is no significant different of the oxygen concentration after 1200 s. Similar as oxygen, glucose weight percentage showed a plat trend since 1200 s, given Fig. 5b. The reason is that bottom layer is closer to the nutrient injection area (bottom surface) compare to other layers and the layer 1 is far away of the injection surface. All 4 layers is surrounded by cylinder surrounding injection surface which means that the only reason that cause nutrient concentration different is the bottom surface injection.

3.3 Oxygen and Glucose Transportation Path

In the whole simulation process, with a faster diffusion speed than oxygen, glucose could be transformed into the middle of the scaffold deeply. As it shown in Fig. 6, the scaffold section is separated by 16 parts. According the counter images showed below, it showed that the transportation path very clear that oxygen and glucose was first fulfil the area 1 and 4. Then, they would be transported to area 2,3,5 and 8. After that, they are moving to area 6, 7, 13 and 16 which the nutrients density grow more quickly in area 13 and 16 than 6 and 7. At the end, oxygen and glucose will transport to area 10 and 11 before moving to the area 14 and 15.

As the image shown in Fig. 7b, the black spots represent the cells that are already attached on the scaffold [22]. The cells attachment process is governed by cell imping-ing model which include 4 impinge regimes (stick, spread, splash and rebound) [22]. The Fig. 7a showed how much oxygen and glucose that cells could be able to absorb. It is showed that glucose is nearly saturated after 1600 s. In contrast, the oxygen remains a steady increasing trend from initial until 2000s. The reason is that glucose reached saturation faster than oxygen because the diffusion speed of oxygen is far lower than glucose.

3.4 Effects on Bone Distribution

To validate the numerical model, the simulation results are compared with in vivo tests which quantified regenerated bone tissue by MATLAB image analysis program through micro CT and CT images which has been illustrated on previous research. The scaffold infiltrated into the blood part could be separated into 4 layers shown in Fig. 3.

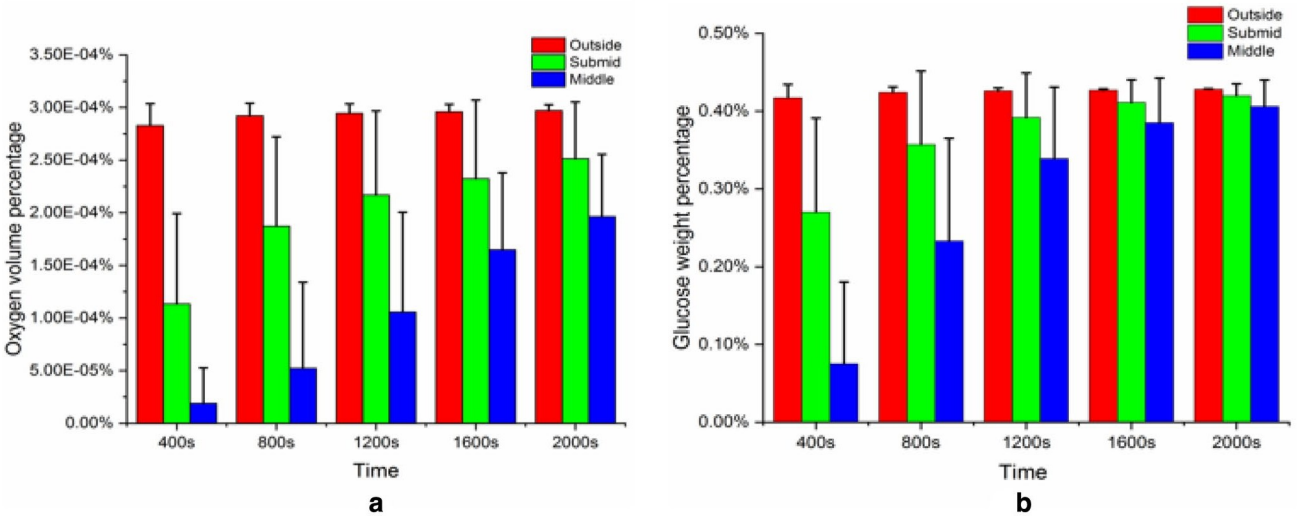

Fig. 4 Oxygen and glucose distribution in horizontal view (**a** oxygen distribution; **b** glucose distribution)

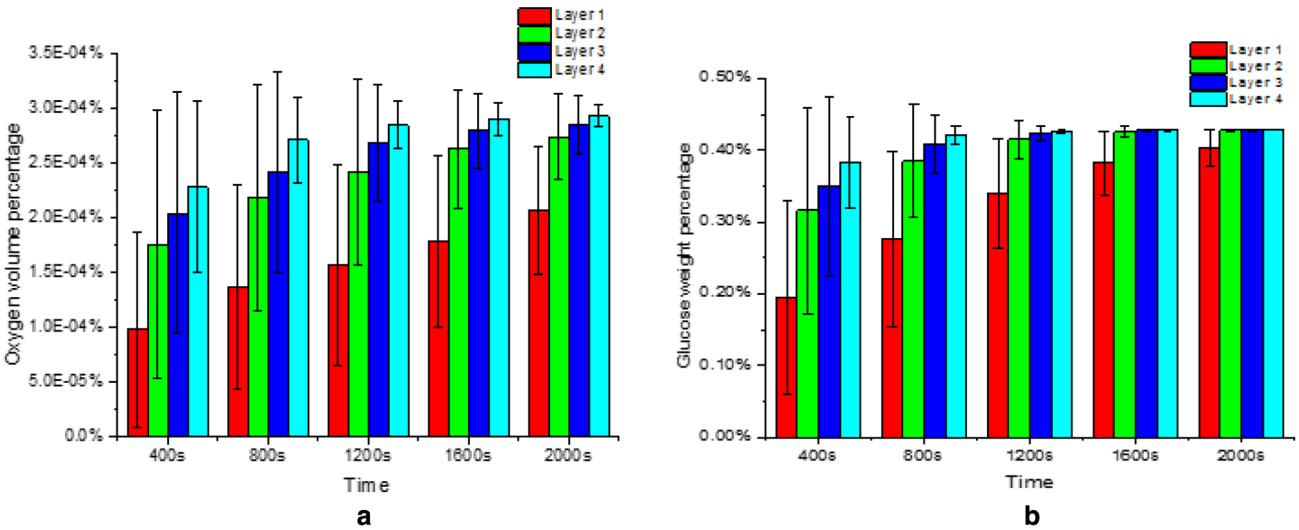

Fig. 5 Oxygen and glucose distribution in vertical view (**a** oxygen distribution; **b** glucose distribution)

According to the vertical analysis of regenerated bone tissue, there is a slightly decreasing from bottom to top surface and there is almost no difference between two middle layers of the new bone formation. The regenerated bone tissue distribution in vertical is more similar to the oxygen distribution in vertical than glucose.

The simulation results at 2000s showed that the glucose distribution between the top 3 layers is nearly the same value which is around 0.428% except the bottom one which is only 0.404%, given in Fig. 8. Oxygen diffusivity in the fluid is 2×10^{-9} cm^2/s while glucose diffusivity in the fluid is 9.2×10^{-7} cm^2/s.

Unlike the glucose distribution, oxygen distributed at the top layer above 2E-4% but reached nearly 3E-4% on the bottom. It showed a gradual decreasing trend from bottom to top and oxygen distributed in the two middle layers are nearly the same. The distribution trend of oxygen more likely fit the bone distribution curve.

4 Discussion

According to the simulation results comparing with the new bone tissue regeneration in vivo test, oxygen distribution showed a more similar trend as bone tissue regeneration,

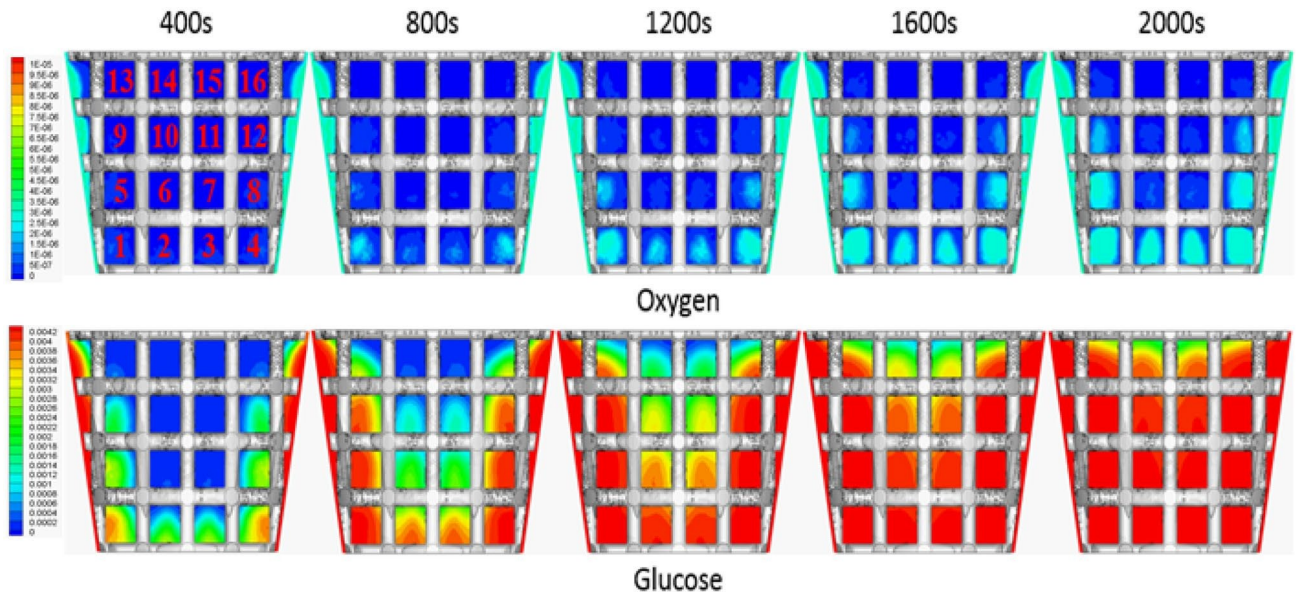

Fig. 6 Oxygen and glucose transportation process

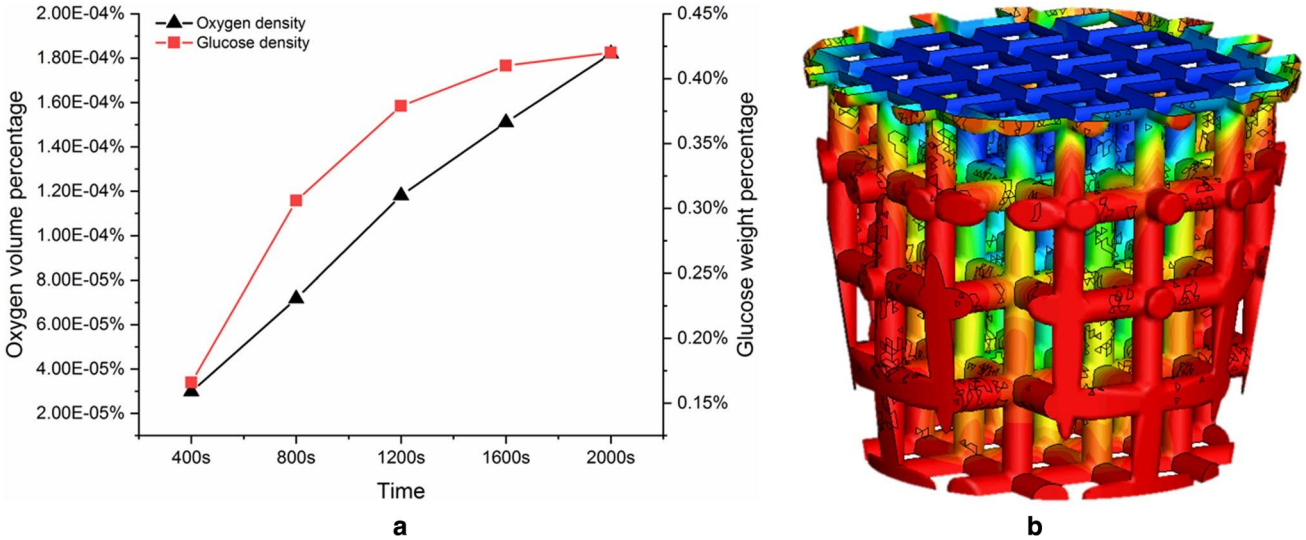

Fig. 7 Oxygen and glucose transport comparison and cells absorption schematic diagram

which indicated that oxygen concentration made an important role in bone tissue regeneration. This result is also in agreement with Dunn et al. [24] that this growth pattern is depended on oxygen diffusion.

In recent years, several researchers found that cell density decreased towards the centre of the scaffold but maintain a high density in 1 mm or less from the edge [25, 26]. The oxygen concentration is also founded that it has similar trend as well. According to simulation results, oxygen concentration showed a more similar trend increasing when time goes by than glucose. It is shown that after 2000s, glucose nearly distributed the whole scaffold system. Although there is no agreement that what is the accurate diffusion rate of glucose and oxygen is, all references showed that glucose diffusion speed is far higher than the oxygen diffusion [24, 27, 28]. In that case, it would take a really 1 h or more for oxygen to reach the centre of the scaffold.

However, in the real biosystem, the transportation speed would be much lower than expect. Blood is a semi-solid tissue which could be found in trabecular bone. There is no doubt that blood will start solidify after putting the scaffold into the target area. This is known as wound healing process

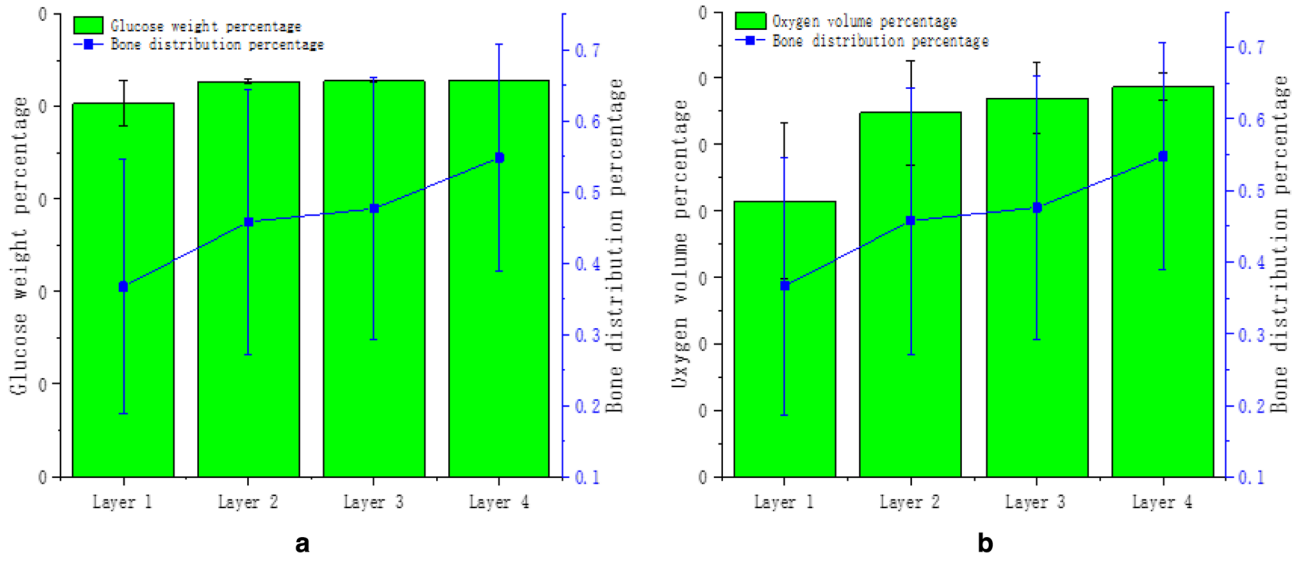

Fig. 8 Comparison of glucose weight percentage and bone distribution percentage (2000s); Comparison of oxygen volume percentage and bone distribution percentage (2000s)

which begins at the onset of injury, and the objective is to stop the bleeding. At the beginning, blood is more likely a type of fluid which could act as a medium to carry nutrients into the system. In other words, oxygen and glucose transportation are governed by 2 types of speeds when blood act as a fluid medium which are inlet speed and diffusion speed. After a period of time, bone marrow would start to solidify which means that nutrients transportation type would only limit to diffusion. The reason is that particles in the solid are not able to move from one place to another which means that convection does not happen in solid. The diffusive ability of the nutrients would decrease along with the solidify process. Meanwhile, as the cells begin to proliferate and differentiate, more nutrients are needed in the system. However, not enough nutrients could be taken into the middle of the scaffold. The cells attached on the scaffold edge side will growth far more quickly than the middle which will cause more regenerated bone tissue on the outside than in the middle. The diffusion is further reduced as external cell growth block the flow access. That is the main reason to broaden internal connect access in scaffold design.

Based on in vivo results, it is achieved that 30% of regenerated bone growing in the middle of the scaffold after 3 months in vivo tests which demonstrated that scaffold could supply a good nutrient transportation [24–26]. The reason is that 3D printed scaffold structure has a good interconnectivity and lots of nutrients transportation channels which shortens the transportation distance from outside of the scaffold to the middle.

There are still needs to further study this simulation settings. First, there is lack the detail understanding how the nutrients achieve transportation after the bone marrow solidifies and how long does it take. Thus, the 2000s simulation time is just an assumption. It is assumed that after 2000s, the bone marrow would start solidify. Second, when bone marrow flow into the system after putting the scaffold in the targeting area, it will carry BMSCs and nutrients into the system simultaneously. There is no evidence shows how much concentration that oxygen and glucose have and how they perform during that short period of time. In that case, an assumption is made to simplify the model which is that all nutrients flowed into the system at that short period time was absorbed by the cells. In other words, before this simulation start, no more nutrients distribute in the whole system. Further, many other factors need to be quantified and put into this model such as metabolic wastes, cell–cell signalling molecules, growth factors, and cell chemotactic factors in the future [19].

5 Conclusion

This numerical model, validated by the previous in vivo studies, provides an opportunity to predict and understand nutrient transportation in the animal or human body. In comparison to the simulation results, the oxygen distribution at the initial stage was similar to that of bone formation in the scaffold. It is found that oxygen concentration played a very important role in bone tissue regeneration, with lower concentrations than glucose in the system. The model is only available to predict nutrient transport in initial 2000s as blood would begin to solidify shortly afterwards. After this process, the nutrient transport method should only be dependent upon diffusion which should be investigated in

the future. Although there are a lot of factors that influence bone formation, nutrient transport is one of the important factors as lower concentrations would cause less tissue regeneration. This model could also help researchers reduce the number of in vitro and in vivo test for optimizing osteochondral scaffold structures. Compared to other scaffold manufacturing methods, additive manufacturing is an easy and simple method to design good interconnective osteochondral scaffolds for optimal nutrient transportation. As the diffusion could be further reduced by cell growth at the external area, novel structures should be made in the future to avoid the cells growing at external side and thus blocking the nutrients access into the scaffold.

Funding This work was supported by Versus Arthritis UK (Grant no: 21977); European Commission via a H2020-MSCA-RISE programme (BAMOS, Grant no: 734156); Innovative UK via Newton Fund (Grant no: 102872); Engineering and Physical Science Research Council (EPSRC) via DTP CASE programme (Grant no: EP/T517793/1).

Declarations

Conflict of interests The authors declare that there are no conflicts of interest.

References

1. Karageorgiou, V., & Kaplan, D. (2005). Porosity of 3D biomaterial scaffolds and osteogenesis. *Biomaterials, 26*, 5474–5491.
2. Huiskes, R., van Driel, W. D., Prendergast, P. J., & Søballe, K. (1997). A biomechanical regulatory model for periprosthetic fibrous-tissue differentiation. *Journal of Materials Science: Materials in Medicine, 8*, 785–788.
3. Tamaddon, M., Chen, S. M., Vanaclocha, L., Hart, A., El-Husseiny, M., Henckel, J., & Liu, C. (2017). Decrease in local volumetric bone mineral density in osteoarthritic joints is associated with the increase in cartilage damage: A peripheral quantitative CT study. *Frontiers in Materials, 4*, 37.
4. Tamaddon, M., Samizadeh, S., Wang, L., Blunn, G., & Liu, C. (2017). Intrinsic osteoinductivity of porous titanium scaffold for bone tissue engineering. *International Journal of Biomaterials, 2017*, 5093063.
5. Tamaddon, M., Blunn, G., & Liu, C. (2016). 3D printed PLA/collagen hybrid scaffolds for bone-cartilage interface tissue engineering. *European Cells and Materials, 32*, 113.
6. Karande, T. S., Ong, J. L., & Agrawal, C. M. (2004). Diffusion in musculoskeletal tissue engineering scaffolds: Design issues related to porosity, permeability, architecture, and nutrient mixing. *Annals of Biomedical Engineering, 32*, 1728–1743.
7. Huang, H., Liu, C., Yi, T., Tamaddon, M., Yuan, S., Shi, Z., & Liu, Z. (2021). Substitution for in vitro and in vivo tests: Computational models from cell attachment to tissue regeneration. *Chinese Medical Sciences Journal, 36*, 323–332.
8. Mofrad, A. Z., Mashayekhan, S., & Bastani, D. (2017). Simulation of the effects of oxygen carriers and scaffold geometry on oxygen distribution and cell growth in a channeled scaffold for engineering myocardium. *Mathematical Biosciences, 294*, 160–171.
9. Lee, M., Dunn, J. C. Y., & Wu, B. M. (2005). Scaffold fabrication by indirect three-dimensional printing. *Biomaterials, 26*, 4281–4289.
10. Freed, L. E., Marquis, J. C., Langer, R., Vunjak-Novakovic, G., & Emmanual, J. (1994). Composition of cell-polymer cartilage implants. *Biotechnology and Bioengineering, 43*, 605–614.
11. Carrier, R. L., Rupnick, M., Langer, R., Schoen, F. J., Freed, L. E., & Vunjak-Novakovic, G. (2002). Effects of oxygen on engineered cardiac muscle. *Biotechnology and Bioengineering, 78*, 617–625.
12. Murphy, C. L., & Polak, J. M. (2004). Control of human articular chondrocyte differentiation by reduced oxygen tension. *Journal of Cellular Physiology, 199*, 451–459.
13. Murphy, C. L., & Sambaniss, A. (2001). Effect of oxygen tension on chondrocyte extracellular matrix accumulation. *Connective Tissue Research, 42*, 87–96.
14. Rouwkema, J., Koopman, B. F. J. M., Van Blitterswijk, C. A., Dhert, W. J. A., & Malda, J. (2009). Supply of nutrients to cells in engineered tissues. *Biotechnology and Genetic Engineering Reviews, 26*, 163–178.
15. Liu, Z., Tao, C., Yuan, S., Wang, W., Tamaddon, M., Ng, L., Huang, H., Sun, X., & Liu, C. (2022). Eularian wall film model for predicting dynamic cell culture process to evaluate scaffold design in a perfusion bioreactor. *Medicine in Novel Technology and Devices, 13*, 100104.
16. Reynolds, M., & McCann, S. R. (1985). Human marrow stromal cells in short-term semi-solid bone marrow culture in aplastic anaemia. *Scandinavian Journal of Haematology, 34*, 101–110.
17. Liu, Z., Tamaddon, M., Gu, Y., Yu, J., Xu, N., Gang, F., Sun, X., & Liu, C. (2020). Cell seeding process experiment and simulation on three-dimensional polyhedron and cross-link design scaffolds. *Frontiers in Bioengineering and Biotechnology, 8*, 104.
18. Xu, S., Du, P., Xie, Y., & Yue, Y. (2008). Cell distribution in a scaffold with random architectures under the influence of fluid dynamics. *Journal of Biomaterials Applications, 23*, 229–245.
19. Botchwey, E. A., Dupree, M. A., Pollack, S. R., Levine, E. M., & Laurencin, C. T. (2003). Tissue engineered bone: Measurement of nutrient transport in three-dimensional matrices. *Journal of Biomedical Materials Research Part A: An Official Journal of The Society for Biomaterials, The Japanese Society for Biomaterials, and The Australian Society for Biomaterials and the Korean Society for Biomaterials, 67*, 357–367.
20. Amini, A. R., Laurencin, C. T., & Nukavarapu, S. P. (2012). Bone tissue engineering: Recent advances and challenges. *Critical Reviews in Biomedical Engineering, 2012*, 40.
21. Byrne, D. P., Lacroix, D., Planell, J. A., Kelly, D. J., & Prendergast, P. J. (2007). Simulation of tissue differentiation in a scaffold as a function of porosity, Young's modulus and dissolution rate: Application of mechanobiological models in tissue engineering. *Biomaterials, 28*, 5544–5554.
22. Liu, Z., Tamaddon, M., Chen, S.-M., Wang, H., San Cheong, V., Gang, F., Sun, X., & Liu, C. (2021). Determination of an initial stage of the bone tissue ingrowth into titanium matrix by cell adhesion model. *Frontiers in Bioengineering and Biotechnology, 9*, 736063.
23. Tamaddon, M., Blunn, G., Xu, W., Alemán Domínguez, M. E., Monzón, M., Donaldson, J., Skinner, J., Arnett, T. R., Wang, L., & Liu, C. (2021). Sheep condyle model evaluation of bone marrow cell concentrate combined with a scaffold for repair of large osteochondral defects. *Bone & Joint Research, 10*, 677–689.
24. Dunn, J. C. Y., Chan, W.-Y., Cristini, V., Kim, J. S., Lowengrub, J., Singh, S., & Wu, B. M. (2006). Analysis of cell growth in three-dimensional scaffolds. *Tissue Engineering, 12*, 705–716.
25. Yu, P. (2012). Numerical simulation on oxygen transfer in a porous scaffold for animal cell culture. *International Journal of Heat and Mass Transfer, 55*, 4043–4052.

26. Makhaniok, A., Haranava, Y., Goranov, V., Panseri, S., Semerikhina, S., Russo, A., Marcacci, M., & Dediu, V. (2013). In silico prediction of the cell proliferation in porous scaffold using model of effective pore. *Bio Systems, 114*, 227–237.
27. Frank, E. H., Grodzinsky, A. J., Phillips, S. L., & Grimshaw, P. E. (1990). *Physicochemical and bioelectrical determinants of cartilage material properties*. In *Biomechanics of diarthrodial joints* (pp. 261–282). Springer, New York.
28. Lin, T., Jhang, H., Chu, F., & Chung, C. A. (2013). Computational modeling of nutrient utilization in engineered cartilage. *Biotechnology Progress, 29*, 452–462.